High-Performance Multifunctional Photodetector and THz Modulator Based on Graphene/TiO2/p-Si Heterojunction

Lichuan Jin (lichuanj@uestc.edu.cn)
University of Electronic Science and Technology of China https://orcid.org/0000-0002-9398-3565
Miaoqing Wei
University of Electronic Science and Technology of China
Dainan Zhang
University of Electronic Science and Technology of China
Lei Zhang
University of Electronic Science and Technology of China
Huaiwu Zhang
University of Electronic Science and Technology of China

Nano Express

Keywords: multifunctional device, graphene/TiO2/p-Si, photodetector, broadband THz wave modulator

Posted Date: April 21st, 2021

DOI: https://doi.org/10.21203/rs.3.rs-443002/v1

Version of Record: A version of this preprint was published at Nanoscale Research Letters on August 21st, 2021. See the published version at https://doi.org/10.1186/s11671-021-03589-w.

Abstract

In this paper, we have prepared a multifunctional device based on graphene/TiO_2/p-Si heterojunction and systematically studied the optical response of the device in the ultraviolet-visible-infrared band and the transmission changes of terahertz waves in the 0.3-1.0 THz band under different bias voltages. As a photodetector, the “back-to-back” p-n-p energy band structure makes the device have a serious unbalanced distribution of photogenerated carriers in the vertical direction when light is incident from the graphene side, which ensures a higher optical gain of the device, so as to achieve a responsivity up to 3.6 A/W and a detectability of 4×10^{13} Jones under 750 nm laser irradiation. As a terahertz modulator, the addition of the TiO_2 layer allows the device to continuously widen the carrier depletion region under negative bias, thereby realizing modulation of the terahertz wave, making the modulation depth up to 23% under − 15 V bias. However, there is almost no change in the transmission of the terahertz wave when positive bias is applied. An analogue of an electronic semiconductor diode effect is realized that allows passage of the terahertz wave only for negative bias and blocks the terahertz wave while positively biased.

Introduction

Photodetector is a type of optoelectronic device that can convert a light signal into an electrical signal and are widely used in optical communications, thermal imaging, environmental monitoring, biomedical imaging, etc. [1–5] And terahertz (THz) broadband modulator is a key device to realize the practical application of terahertz wave in communication, imaging, sensing and other application fields. [6–10] Therefore, the development of a high-speed modulator that works at room temperature, is small in size and easy to process is of great significance to promote the development and practicality of terahertz technology.

Graphene has shown great application value in the field of photodetectors and terahertz modulators due to its special energy band structure and ultra-high carrier mobility. [11–16] Therefore, the realization of multifunctional photodetectors and terahertz modulators based on graphene-based heterojunction is also possible, which will be conducive to the miniaturization of electronic communication systems. Graphene-based photodetectors have been extensively studied in the past few years. Graphene/Si heterojunction has high photoelectric conversion efficiency and thus has great potential to obtain high-performance photodetectors. [17–20] However, the low optical absorption of graphene (~ 2.3% for single layer of graphene) results in a low responsivity. [21, 22] The interface between Si and graphene contains a large number of surface states pinning the surface Fermi level, leading to a strong leakage current noise. Therefore, various methods for improving the performance of graphene/silicon photodetectors have been proposed, including insertion of interfacial oxide layer, silicon waveguide integration, optical absorption layer addition, surface plasmon enhancement.[23–29]

For graphene-based terahertz modulators, both optical pump and external voltage bias can be used as excitation signals. In 2014, Wen et al. [30] proposed a modulator in which a layer of graphene is laid on a germanium substrate to perform all-optical modulation of terahertz waves. When the sample was irradiated with a 1550 nm communication wavelength laser in the test, the terahertz transmission intensity dropped sharply as the laser power increased. In the frequency range of 0.25-1 THz, the modulation depth reaches 94%. In 2012, Professor Sensale et al. [31] used a graphene-based field effect transistor (GFET) with 92 nm SiO_2 as the dielectric layer to make a terahertz modulator with a modulation depth of 15% and a modulation rate of 18Kb/s. Such a THz wave wide-band modulator completely uses the electron and hole concentration changes in the graphene film to control the attenuation of the terahertz wave energy. After that, aluminum oxide Al_2O_3, YIG and other materials [32–34] can effectively reduce the Coulomb scattering and cavity effect of graphene due to their high dielectric constant, and thus are used as the dielectric layer of the GFET terahertz wave modulator.

In this study, a graphene/TiO_2/p-Si trilayer heterojunction was fabricated, which can be performed as a photodetector and a broadband THz wave modulator. Moreover, the device we designed can also work as a diode for terahertz waves, which allows passage of current only for negative bias and blocks the current when positively biased.

Methods

The prototype of the multifunctional photodetector and THz modulator based on graphene/TiO_2/p-Si heterojunction is shown in Fig. 1. The TiO_2 film was deposited on the p-Si substrate (500-μm-thick, resistivity ρ ~ 1–10 Ω cm) by low temperature hydrothermal method. The cleaned silicon substrate was immersed into 0.1 M $TiCl_4$ aqueous solution at 343 K for one hour to obtain about 10 nm-thick TiO_2 film. The monolayer graphene grown on the copper substrate by chemical vapor deposition [35] was spin-coated with PMMA and immersed into 1mol/L $FeCl_3$ solution to remove the copper background. After that, the TiO_2/p-Si substrate was used to pick up the PMMA-coated monolayer graphene and then dry it. Then immerse PMMA-coated graphene/ TiO_2/p-Si substrate in acetone solution to remove PMMA [36], and obtain graphene/TiO_2/p-Si trilayer heterojunction. The photoresponses of the graphene/TiO_2/p-Si heterojunction, including photogenerated current and time-dependent characteristics, were measured with a monochromator (Zolix, Omni-λ 300i), which use order sorting filters to provide white and monochromatic light. The I-V curves and I-t curves of the graphene/TiO_2/p-Si heterojunction under light illumination were measured by a SourceMeter (Keithley 2601B). The terahertz wave transmission was measured by a Fico THz time domain system (Zomega Terahertz Corporation).

Results And Discussion

Figure 2(a) shows the dark current of the device and the photocurrent when excited by white light changes with the bias voltage, and the change of the current with voltage when 2 Hz white light is applied. It can be seen from the Fig. 2(a) that the device has obvious rectification effect. The positive direction of the applied voltage is from the silicon side to the graphene side, which indicates that the main built-in electric field of the device comes from the silicon-titanium oxide junction, and the built-in electric field constructed by weak p-type graphene and weak n-type TiO_2 can be ignored. Under the negative bias voltage, the built-in electric field is further enhanced by the external bias voltage. Light is incident from the graphene side, and a large number of photogenerated carriers

are collected by the graphene and quickly transmitted out, which results in an imbalance between the photo-generated carriers on the graphene side and the silicon side, thereby obtaining a strong optical guide gain under high bias. When 2 Hz white light is applied, the current coincides with the dark current when no light is applied, and coincides with the photocurrent when light is applied, which shows that the device has a high response speed and good repeatability. As shown in Fig. 2(b), graphene/TiO_2/p-Si has obvious photoelectric response under light from 350 nm to 1050 nm wavelength at a bias of -2 V. It can be seen from the figure that the dark current of the device does not change much under different wavelengths of laser irradiation. However, the dark current increases slightly with the increase of time, which is caused by the heat loss when the device is working. As the working time of the device is extended, there is a local temperature rise, which causes the increase of the leakage current. The photocurrent of the device change obviously under different light waves (350 nm-1050 nm). The photoresponse currents (I_{on}-I_{off}) at 350 nm, 550 nm, 750 nm, 950 nm and 1050 nm are 126.29, 213.35, 189.67, 335.93, and 102.46 μA, respectively.

Figure 3(a) and Fig. 3(b) exhibits the spectra-dependent of Responsivity (R), external quantum efficiency (EQE) and Detectivity (D*) of the heterojunction. R, EQE and D* are important parameters to evaluate the performance of photodetectors. Responsivity (R) is defined as $R=(I_{on}-I_{off})/P_{in}$, where I_{on}, I_{off} and P_{in} are photocurrent, dark current and incident light power. External quantum efficiency (EQE) refers to the number of electron-hole pairs excited by the unit incident photon, which reflects the sensitivity of photodetectors to photons and can be calculated as EQE = Rhc/λ, where h, c and λ are Plank's constant, elementary charge and wavelength of incident light, respectively. Detectivity (D*) can be expressed as $D^* = R/(2qI_d/A)^{1/2}$, where I_d is the dark current and A is active area (0.5 cm^2). The highest responsivity and EQE of 3.6 A/W and 6001% was observed under light with 0.417 mW/cm^2 intensity and 750 nm wavelength. Detectivity is 4×10^{13} Jones at 750 nm light, about 520 times higher than the graphene/Si photodetector. [37] Light is incident from the graphene side, and the carriers excited by the short-wavelength are near the TiO_2 side. At this time, the electrons are quickly collected by the graphene under the negative bias voltage. However, holes need to travel a long distance before received by the electrode on the silicon side, which causes serious recombination and reduces the photoresponse of the device. Insufficient absorption of long-wavelength light by Si will also reduce the photoresponse of the device. The excitation light near 750 nm wavelength can be completely absorbed by Si, and the distribution of photogenerated carriers in the thickness direction of the device is relatively uniform, so the best responsivity is obtained.

The THz wave transmittance of the THz wave of the graphene/TiO_2/p-Si heterojunction in the range of 0.3 to 1 THz is shown in Fig. 4(a). It can be seen from the Fig. 4(a) that when a positive bias voltage of 5 V and 10 V is applied, the transmittance of the THz wave hardly changes compared to 0 V. When negative bias voltages of -10 V, -15 V, and − 20 V are applied, the THz wave transmittance changes significantly. The direction of the applied negative bias electric field is consistent with the direction of the built-in electric field of p-Si and TiO_2. As the negative bias voltage increases, the space charge region widens, and the device gradually becomes fully depleted. Meanwhile, there is no carrier accumulation inside the device, the carriers move in the external circuit, and the transmission of the terahertz wave increases. Modulation depth is an important performance parameter of terahertz modulators,which can be calculated by $(T_{excitation} - T_{no\ excitation})/T_{no\ excitation}$, where the $T_{excitation}$ and $T_{no\ excitation}$ represent the intensity of THz transmission with and without photoexcitation respectively. The variation of the modulation depth of the device under different bias voltages in the range of 0.3-1.0 THz is calculated, and the result is shown in Fig. 4(b). It can be seen from the figure that when 5 V and 10 V are applied, the modulation depth is approximately zero. The modulation depth is about 23% at -15 V. At -20 V, the modulation depth decreases slightly, about 22.6%. This is because when the voltage is extremely high, the device will break down in the reverse region and the current will increase. Continuing to increase the voltage will not further broaden the space charge layer to increase THz transmission, but will increase the temperature of the device and increase the carrier concentration due to the thermal effect caused by the increase in current, which cause the decrease of the terahertz wave, resulting in the decrease of the modulation depth.

The time-domain signals of the graphene/TiO_2/p-Si THz modulator with various bias voltages are plotted in Fig. 5(a). We can see that the time-domain graph when positive gate voltage is applied almost coincides with the graph when 0 V is applied. When a negative bias is applied, the THz transmission peak increases significantly. The peak value at 0, 5, 10, -10, -15 and − 20 V is about 72.49, 73.39, 72.49, 79.7 88.66 and 87.15 respectively. In order to show this change more intuitively, we plot the change of the device's terahertz transmission peak under different voltages in Fig. 5(b). It is clear that the device allows terahertz waves to pass under negative bias, but prevents terahertz waves from passing under positive bias. It represents that our terahertz modulator can also function as a diode for terahertz waves.

Conclusions

In summary, the graphene/TiO_2/p-Si heterojunction can perform as both a high-performance photodetector and a broadband THz wave modulator. The device has obvious light response in the ultraviolet-visible-infrared band. And the responsivity, external quantum efficiency and detectivity are as high as 3.6 A/W, 6001% and 4×10^{13} Jones under 0.417 mW/cm^2 density and 750 nm wavelength laser irradiation. What's more, the transmission modulation depth of the terahertz wave can reach up to 23% in the broadband of 0.3-1.0 THz when biased with a -15 V negative voltage. While there is almost no change in the transmission of the terahertz wave under a positive voltage, which represents that the device can function as "a diode" relative to the terahertz wave.

List Of Abbreviations

Terahertz (THz)

graphene-based field effect transistor (GFET)

Responsivity (R),

External quantum efficiency (EQE)

Detectivity (D*)

Declarations

Acknowledgements

None

Funding

This work was supported by the National Natural Science Foundation of China under Grant No. 51702042, National Key Research and Development Plan unde

Author's Contributions

MQW conceived the idea, fabricated the devices, and wrote the paper. LZ contributed to the sample fabrication. DNZ and LCJ analyzed the data. HWZ supervised the paper. All authors read and approved the manuscript.

Competing Interests

The authors declare no competing interests.

Availability of data and material

All data supporting the conclusions of this article are included within the article.

Authors' information

All authors: School of Electronic Science and Engineering (National Exemplary School of Microelectronics), University of Electronic Science and Technology of China, Chengdu 611731, China

DNZ, LCJ and HWZ: State Key Laboratory of Electronic Thin Films and Integrated Devices, University of Electronic Science and Technology of China, Chengdu 611731, China

References

1. Koppens FHL, Mueller T, Avouris P, et al (2014) Photodetectors based on graphene, other two-dimensional materials and hybrid systems. Nat Nanotechnol 9:780–793.
2. Kang P, Wang MC, Knapp PM, Nam SW (2016) Crumpled Graphene Photodetector with Enhanced, Strain-Tunable, and Wavelength-Selective Photoresponsivity. Adv Mater 28:4639–4645.
3. Cao F, Liao Q, Deng K, et al (2018) Novel perovskite/TiO2/Si trilayer heterojunctions for high-performance self-powered ultraviolet-visible-near infrared (UV-Vis-NIR) photodetectors. Nano Res 11:1722–1730.
4. Sun H, Tian W, Cao F, et al (2018) Ultrahigh-Performance Self-Powered Flexible Double-Twisted Fibrous Broadband Perovskite Photodetector. Adv Mater 30:1706986.
5. Hu X, Zou P, Yin Z, et al (2020) Hot-Electron Photodetection Based on Graphene Transparent Conductive Electrode. IEEE Sens J 20:6354–6358.
6. Wen T, Zhang D, Wen Q, et al (2016) Enhanced Optical Modulation Depth of Terahertz Waves by Self-Assembled Monolayer of Plasmonic Gold Nanoparticles. Adv Opt Mater. 4:1974
7. Sun Z, Martinez A, Wang F (2016) Optical modulators with 2D layered materials. Nat Photonics 10:227–238.
8. Yang DS, Jiang T, Cheng XA (2017) Optically controlled terahertz modulator by liquid-exfoliated multilayer WS_2 nanosheets. Opt Express 25:16364.
9. Qiao J, Wang S, Wang Z, et al (2020) Ultrasensitive and Broadband All-Optically Controlled THz Modulator Based on $MoTe_2$/Si van der Waals Heterostructure. Adv Opt Mater 8:2000160.
10. Degl'Innocenti R, Kindness SJ, Beere HE, Ritchie DA (2018) All-integrated terahertz modulators. Nanophotonics 7:127–144.
11. Hu M, Yan Y, Huang K, et al (2018) Performance Improvement of Graphene/Silicon Photodetectors Using High Work Function Metal Nanoparticles with Plasma Effect. Adv Opt Mater 6:1701243.
12. Kang B, Kim Y, Yoo WJ, Lee C (2018) Ultrahigh Photoresponsive Device Based on ReS_2/Graphene Heterostructure. Small 14:1802593.
13. Wei X, Yan F, Lv Q, et al (2017) Fast gate-tunable photodetection in the graphene sandwiched WSe2/GaSe heterojunctions. Nanoscale 9:8388–8392.
14. Shi YX, Li JS, Zhang L (2017) Graphene-integrated split-ring resonator terahertz modulator. Opt Quantum Electron 49:350.
15. Chen Z, Chen X, Tao L, et al (2018) Graphene controlled Brewster angle device for ultra broadband terahertz modulation. Nat Commun 9:4909.
16. Kakenov N, Ergoktas MS, Balci O, Kocabas C (2018) Graphene Based Terahertz Phase Modulators. 2D Mater 5:035018
17. Wang Y, Ding K, Sun B, et al (2016) Two-dimensional layered material/silicon heterojunctions for energy and optoelectronic applications. Nano Res 9:72–93.
18. Bartolomeo A Di, Luongo G, Giubileo F, et al (2017) Hybrid Graphene/Silicon Schottky photodiode with intrinsic gating effect. 2D Mater 4:025075
19. Tian W, Wang Y, Chen L, Li L (2017) Self-Powered Nanoscale Photodetectors. Small 13:1701848.
20. Lin S, Lu Y, Xu J, et al (2017) High performance graphene/semiconductor van der Waals heterostructure optoelectronic devices. Nano Energy 40:122–148.

21. Nair RR, Blake P, Grigorenko AN, et al (2008) Fine structure constant defines visual transparency of graphene. Science 320:1308.
22. Lv P, Zhang X, Zhang X, et al (2013) High-Sensitivity and Fast-Response Graphene / Crystalline Silicon Schottky. IEEE Electron Device Lett 34:1337–1339
23. Yan F, Wei Z, Wei X, et al (2018) Toward High-Performance Photodetectors Based on 2D Materials: Strategy on Methods. Small Methods 2:1700349.
24. An J, Wang B, Shu C, et al (2020) Research development of 2D materials based photodetectors towards mid-infrared regime. Nano Sel 527–540.
25. Yu X, Li Y, Hu X, et al (2018) Narrow bandgap oxide nanoparticles coupled with graphene for high performance mid-infrared photodetection. Nat Commun 9:4299.
26. Du B, Lin L, Liu W, et al (2017) Plasmonic hot electron tunneling photodetection in vertical Au–graphene hybrid nanostructures. Laser Photonics Rev 11:1600148.
27. Shao D, Gao J, Chow P, et al (2015) Organic-Inorganic Heterointerfaces for Ultrasensitive Detection of Ultraviolet Light. Nano Lett 15:3787–3792.
28. Li X, Zhu M, Du M, et al (2016) High Detectivity Graphene-Silicon Heterojunction Photodetector. Small 12:595–601.
29. Ma P, Salamin Y, Baeuerle B, et al (2019) Plasmonically Enhanced Graphene Photodetector Featuring 100 Gbit/s Data Reception, High Responsivity, and Compact Size. ACS Photonics 6:154–161.
30. Wen QY, Tian W, Mao Q, et al (2014) Graphene based all-optical spatial terahertz modulator. Sci Rep 4:7409.
31. Sensale-Rodriguez B, Yan R, Kelly MM, et al (2012) Broadband graphene terahertz modulators enabled by intraband transitions. Nat Commun 3:780
32. Mao Q, Wen QY, Tian W, et al (2014) High-speed and broadband terahertz wave modulators based on large-area graphene field-effect transistors. Opt Lett 39:5649.
33. Zhang D, Jin L, Wen T, et al (2017) Manufacturing and terahertz wave modulation properties of graphene/Y3Fe5O12/Si hybrid nanostructures. Compos Part B Eng 111:10–16.
34. Zhang D, Wei M, Wen T, et al (2017) Infrared Properties and Terahertz Wave Modulation of Graphene/MnZn Ferrite/p-Si Heterojunctions. Nanoscale Res Lett 12:482.
35. Li X, Cai W, An J, et al (2009) Large-area synthesis of high-quality and uniform graphene films on copper foils. Science 324:1312–1314.
36. Li X, Zhu Y, Cai W, et al (2009) Transfer of large-area graphene films for high-performance transparent conductive electrodes. Nano Lett 9:4359–4363.
37. An X, Liu F, Jung YJ, Kar S (2013) Tunable graphene-silicon heterojunctions for ultrasensitive photodetection. Nano Lett 13:909–916.

Figures

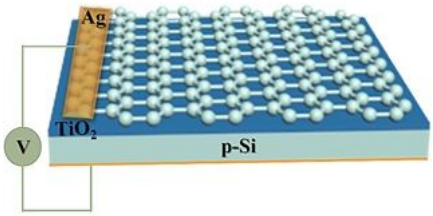

Figure 1

Schematic of the graphene/TiO2/p-Si heterojunction-based multifunctional device

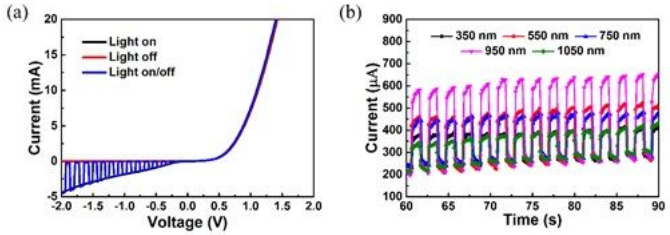

Figure 2

The photoresponse measurements. (a) IV and time-dependent IV curves of the graphene/TiO2/p-Si heterojunction. (b) It curves of the graphene/TiO2/p-Si heterojunction under light of various wavelengths

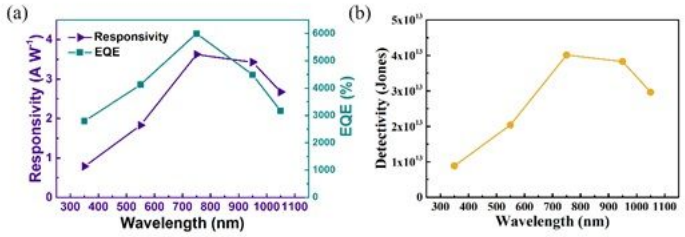

Figure 3

the performance of the graphene/TiO2/p-Si heterojunction. (a) The spectra-dependent responsivity and external quantum efficiency of the graphene/TiO2/p-Si heterojunction. (b) The spectra-dependent detectivity of the graphene/TiO2/p-Si heterojunction

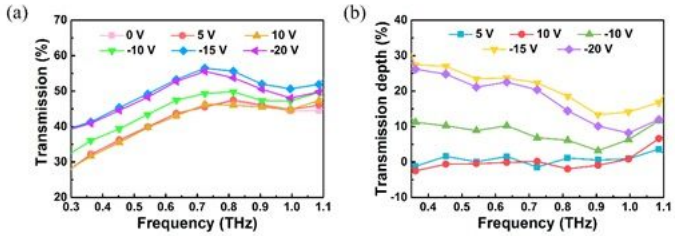

Figure 4

The modulation test. (a) The transmittance spectra of the graphene/TiO2/p-Si at various gate bias voltages. (b) The transmission modulation depth as functions of voltage for graphene/TiO2/p-Si heterojunction.

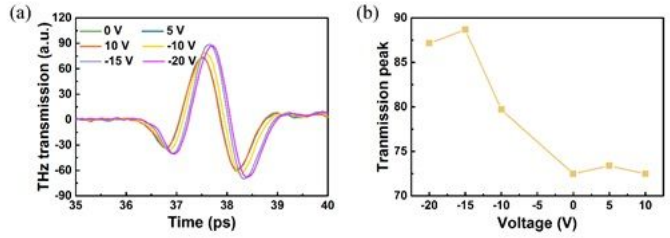

Figure 5

The terahertz time-domain signals. (a) The terahertz time-domain signals at various gate bias voltages. (b) Gate voltage-dependent time-domain terahertz transmission peaks of the graphene/TiO2/p-Si